Carbohydrate Polymer Technologies and Applications 11 (2025) 100895

Contents lists available at ScienceDirect

Carbohydrate Polymer Technologies and Applications

journal homepage: www.sciencedirect.com/journal/carbohydrate-polymer-technologies-and-applications

Electrospun polycaprolactone membranes functionalized with nanochitin for enhanced bioactivity in localized cancer photodynamic therapy

Sofia M. Costa [a,*], Bruno D. Mattos [b], Ricardo C. Calhelha [c], Ya Zhu [b], Eurico Lima [d], Lucinda V. Reis [d,e], Orlando J. Rojas [b,f], Raul Fangueiro [a], Diana P. Ferreira [a,*]

[a] Centre for Textile Science and Technology (2C2T), University of Minho, 4800–058 Guimarães, Portugal
[b] Department of Bioproducts and Biosystems, School of Chemical Engineering, Aalto University, Vuorimiehentie 1, Espoo FI-00076, Finland
[c] CIMO, LA SusTEC, Instituto Politécnico de Bragança, Campus de Santa Apolónia, 5300-253 Bragança, Portugal
[d] Chemistry Centre of Vila Real (CQ-VR), University of Trás-os-Montes and Alto Douro, Quinta de Prados 5001-801, Vila Real, Portugal
[e] Chemistry Department, University of Trás-os-Montes and Alto Douro, Quinta de Prados 5001-801, Vila Real, Portugal
[f] Bioproducts Institute, Department of Chemical and Biological Engineering, Department of Chemistry and Department of Wood Science, University of British Columbia, Vancouver British Columbia V6T 1Z4, Canada

ARTICLE INFO

Keywords:
Electrospinning
Electrospraying
Localized drug delivery systems
Biodegradable polymers
Cancer photodynamic therapy

ABSTRACT

The encapsulation of photosensitizers (PSs) in electrospun membranes has emerged as a promising approach in photodynamic therapy (PDT) on tumor sites, overcoming the drawbacks associated with systemic administration. In this work, localized implants for cancer treatment using PDT were developed by incorporating EL-2 squaraine into poly(ε-caprolactone) (PCL) electrospun microfibers. The latter were coated with chitin nanocrystals (ChNC) by electrospraying, which may improve the biocompatibility and bioactivity of the developed membranes, potentially enhancing the clinical outcomes. The developed electrospun membranes were characterized by water contact angle, imaging, and spectroscopy techniques. The uniform encapsulation and distribution of EL-2 within the microfibers were confirmed while ChNC endowed the membranes with surface hydrophilicity. EL-2 alone displayed about 20 times more cytotoxicity after irradiation compared to the dark condition against HeLa cervical carcinoma cells. Meanwhile, the photodynamic action of PCL+EL-2/ChNC membranes promoted a significant inhibition of cancer cells' proliferation under irradiation, achieving 66.25 % of inhibition, compared to only 24.78 % in dark conditions, using the highest concentration of EL-2. Overall, this work introduces a disruptive strategy using electrospinning-electrospraying to design fibrous therapeutic platforms for cancer PDT, taking advantage of electrospun fibers unique features and the localized nature of photodynamic therapy.

1. Introduction

Cancer continues to stand as one of the foremost global causes of death, claiming around 10 million lives in 2022 (W.H.O. (WHO) 2022). The significance of advanced therapeutic alternatives cannot be overstated, as they have the potential to enhance treatment effectiveness while mitigating conventional treatments' adverse effects. PDT known as a minimally invasive and localized therapy that promotes the death of a target tissue, involves the administration of photoactive molecules, commonly called photosensitizers (PSs). These molecules absorb light with specific wavelength ranges and, upon electronic excitation, convert triplet molecular oxygen into reactive oxygen species (ROS). The presence of these species in high concentrations in the cellular environment promotes cell structural and functional failure, destroying the illuminated tissues (Al-Jamal et al., 2025; Friães et al., 2019; Lobo et al., 2023).

Squaraines are a class of potential PSs that have been explored for PDT applications (Lima & Reis, 2022). These compounds generally present strong absorption in the visible red to near-infrared regions (NIR) (600–900 nm), which is within the so-called "phototherapeutic window". This property is one of the most significant advantages of squaraines compared to other classes of dyes, such as porphyrins since visible-NIR radiation has a more remarkable ability to permeate tissues and light scattering is minimized (Algorri et al., 2021; Lima & Reis, 2023). Other properties such as high fluorescence quantum yields and lifetimes and substantial quantum yield conversion of triplet molecular

* Corresponding authors.
E-mail addresses: sofiamcosta@2c2t.uminho.pt (S.M. Costa), diana.ferreira@det.uminho.pt (D.P. Ferreira).

https://doi.org/10.1016/j.carpta.2025.100895

Available online 16 June 2025

oxygen to cytotoxic singlet oxygen encourage their potential use as PDT photosensitizers (Fernandes et al., 2020; Ferreira et al., 2016; Ferreira et al., 2013; Lima et al., 2022).

PSs' incorporation into polymeric substrates has been demonstrated as a suitable strategy to overtake the drawbacks associated with their systemic administration (Alves et al., 2023). Thus, some challenges can be overcome, including the high dose requirement of PS to achieve a consistent uptake in tumors, the low selectivity and solubility of the drug, the loss of the compound before reaching the target tissue, and the difficulty in reaching deep tissues (Ferreira et al., 2016; Ferreira et al., 2016). Moreover, the use of localized delivery systems to carry the PS may allow its localized delivery in the target tissue and avoid excessive drug circulation (Fu et al., 2018).

Various biopolymer-based matrices have been explored to act as drug delivery systems (DDS) for cancer therapy, including polymeric films, wafers, hydrogels, electrospun micro/nanofibers, among others. Micro/nanofibers produced by electrospinning have attracted increasing attention for their potential application as localized DDS. For instance, compared to solvent cast films, electrospun micro/nanofibers exhibit higher surface area and porosity, improved drug loading capacity and encapsulation efficiency, more controlled drug release and enhanced flexibility (Rohani Shirvan et al., 2021; Ghosal et al., 2018). In contrast, while Gliadel® wafers are approved by Food and Drug Administration (FDA) for the localized treatment of brain tumors, they still face several limitations including rigidity, poor drug diffusion, implant dislodgement and the requirement for large resection cavity sizes (Gazaille et al., 2021; Bastiancich et al., 2016). Hydrogels-based formulations also present challenges, particularly in encapsulating hydrophobic drugs and the usual rapidly drug release due to their high-water content and large pore sizes (Hoare & Kohane, 2008; Rafael et al., 2021).

Electrospinning has emerged as a powerful technique to produce micro/nanofibers that can act as DDS due to its scalability, cost-effectiveness, versatility, ease of operation, and ability to control over the morphology of the produced fibers (Gaydhane et al., 2023). Electrospun micro/nanofibers have stood out as effective drug delivery carriers due to their high surface area-to-volume ratio, associated with high drug loading, more efficient drug encapsulation, homogeneous drug distribution within the polymer matrix, high porosity with small pores and interconnectivity, which allows mass transport properties, vast surface functionalization, allowing target-specific drug delivery, flexibility, conformability to adapt to the morphology of the tissue, and control over the drug release profile. One key advantages of using these fibrous membranes is their ability to mimic the structure of extracellular matrix (ECM), which is considered an active element with a critical role in regulating tumor cell properties and behavior instead of being just a passive one, thereby providing a more effective platform for cellular interactions and biological processes (Rohani Shirvan et al., 2021; CeCe et al., 2023; Costa et al., 2022; Ribeiro et al., 2021; Ribeiro et al., 2021; Tabakoglu et al., 2023; Cavo et al., 2020). The possibility to tailor the composition and the structure of micro/nanofibers highlights their versatility to adapt and respond to diverse requirements, providing opportunities for personalized therapy (Costa et al., 2022). The adjustability of these parameters allows the development of controlled release systems, enabling the safe and long-term maintenance of therapeutically effective drug levels (CeCe et al., 2023). Electrospun micro/nanofibers can also be implanted onto or near a specific target, thereby improving the therapeutic efficiency while reducing the side effects on healthy tissues (Tabakoglu et al., 2023; Ahmad Wsoo et al., 2021; Sayin et al., 2019; Tseng et al., 2013).

The development of DDS using biocompatible and biodegradable polymers is essential to reduce the risk of immune responses as well as to facilitate drug release through the carrier's degradation, eliminating the necessity for surgical removal (Alves et al., 2023; Goonoo et al., 2014). Among degradable polymers, poly(ε-caprolactone) (PCL) stands out for its biocompatibility, bioresorsability, and good mechanical properties. However, its inherent hydrophobicity impairs cell-material interaction. One way to improve the cell interactivity of PCL membranes is by surface modification with hydrophilic compounds (CeCe et al., 2023; Costa et al., 2022; Francavilla et al., 2021; Homaeigohar & Boccaccini, 2022; Shen et al., 2023). Electrospraying has been explored as a surface functionalization methodology to achieve homogeneous coatings by generating charged droplets that are driven toward the substrate by electrostatic forces (Chng et al., 2019; Araújo et al., 2024). This methodology generally uses nanomaterial dispersions instead of polymeric dope solutions (Francis & Hilal, 2022). Chitin, mostly found in the exoskeletons of crustaceans, exhibits biological activity, minimal allergenicity, biocompatibility, biodegradability, and easy processability. Chitin nanocrystals (ChNC), which can be obtained by acid hydrolysis of chitin, have a high surface area, good mechanical properties, and also possess antifungal and antibacterial properties, which prevent biofilm formation on the scaffolds' surface (Bai et al., 2022; Goetz et al., 2016; Wang et al., 2020). In fact, the antimicrobial activity of ChNC is well-documented in the literature, being this effect mainly attributed to the electrostatic interaction between positively charged ChNC and negatively charged microbial cell membranes, resulting in membrane disruption and leakage of intracellular components (Goetz et al., 2016; Jalvo et al., 2017). Additionally, the rod-like structure of these nanocrystals may facilitate their interaction with bacteria, further contributing to the disruption of bacterial cell structures (Xiang et al., 2024). Therefore, the coating of PCL membranes with ChNC by electrospraying is expected to improve the membranes' hydrophilicity as well as to create antimicrobial properties (Goetz et al., 2016; Azimi et al., 2020).

Therefore, considering the potentiality of PDT as therapeutic approach and electrospun micro/nanofibers as localized DDS, the synergistic effect of both has recently emerged as a powerful strategy for targeted and effective cancer therapy (Rohani Shirvan et al., 2021; Ghosal et al., 2018; Costa et al., 2024; Li et al., 2019; Ma et al., 2018; Severyukhina et al., 2016). This study introduces squaraine dye (EL-2) loaded in electrospun PCL microfibers coated with ChNC to act as localized implants for PDT, using electrospinning-electrospraying approach. The photodynamic effect of EL-2 was evaluated using HeLa human cervical carcinoma cell line. The developed samples were characterized by Water Contact Angle (WCA), Field Emission Scanning Electron Microscopy (FESEM), Attenuated Total Reflectance-Fourier Transform Infrared Spectroscopy (ATR-FTIR), UV–visible and fluorescence spectroscopy, Ground State Diffuse Reflectance (GSDR) and Confocal Laser Scanning Microscopy (CLSM). The photodynamic effect of the developed fibrous platforms was assessed by evaluating their *in vitro* dark- and light-cytotoxicity.

2. Materials and methods

2.1. Materials

PCL pellets (molecular weight of 80,000 g/mol), chloroform (CHF) and N,N-dimethylformamide (DMF), sodium hydroxide (NaOH), hydrochloric acid (HCl) and sodium chlorite ($NaClO_2$) were purchased from Sigma Aldrich. Ethanol absolute was provided by VWR.

2.2. Extraction process of ChNC

Chitin nanocrystals (ChNC) were obtained from purified α-chitin obtained from fresh crabs (*Callinectes sapidus*). Crab shells were first cleaned to remove all meat residuals, and then subjected to three cycles of alternated 1 M HCl and 1 M NaOH treatments, with 24 h each. Between each step, the biomass was thoroughly rinsed with distilled water until reaching neutral pH. Then the residual was bleached using a 0.5 wt % $NaClO_2$ solution (pH adjusted to 5 using acetic acid) for 2 h at 70 °C. The purified flakes were ground and stored in wet-state at 4 °C. To obtain the ChNC, never-dried α-chitin flakes were treated with a 33 wt % NaOH solution (12.4 M) at 90 °C for 3 h. This process yielded

deacetylated chitin (degree of deacetylation of 27.3 %, as determined by conductivity titration), which was rinsed with water until pH neutral. Then, deacetylated (DE) chitin was hydrolyzed with HCl to yield ChNC. DE-chitin was treated with 3 M HCl at 95 °C for 1 h. The hydrolysis was stopped by adding a large volume of Mili-Q water (ca. 10 times), followed by centrifugation at 10,000 G for 15 min. The precipitated was collected and dialyzed against Mili-Q water until the pH of the medium reached 3. The last step involved low power tip ultrasonication using on/off alternated cycles to disperse the crystals (Bai et al., 2020).

2.3. Synthesis of squaraine EL-2

EL-2 squaraine dye was synthesized by reacting a solution of 1-hexyl-2,3,3-trimethyl-3*H*-indol-1-ium (4.00 g, 10.8 mmol) and 3,4-dihydroxycyclobut-3-ene-1,2-dione (615 mg, 5.40 mmol) in a mixture of *n*-butanol/pyridine (10 % v/v) under reflux conditions for 5 h. Afterward, the mixture was cooled on an ice bath to enable the precipitation of the product by adding diethyl ether. The resulting residue was then filtered under reduced pressure, washed with distilled water, and subjected to recrystallization from a mixture of dichloromethane and diethyl ether. Bright green crystals were obtained and subsequently dried under reduced pressure. EL-2′s full structural characterization has already been reported by some of us (Lima et al., 2019). Fig. 1 shows the synthesis and chemical structure of squaraine EL-2. The proton and carbon-13 NMR spectra of compound EL-2 are shown in electronic support information (ESI, Fig. S1.1 and S1.2.), confirming its structure.

2.4. In vitro photocytotoxicity of the synthesized squaraine EL-2 on HeLa cell line

The human tumor cell line HeLa (cervical carcinoma) was purchased by DSMZ (Leibniz-Institut DSMZ-Deutsche Sammlung von Mikroorganismen and Zellkulturen GmbH). Cells were routinely maintained as adherent cell cultures in RPMI-1640 medium containing 10 % heat-inactivated FBS, 2 mM glutamine, and 1 % antibiotics at 37 °C, in a humidified air incubator containing 5 % CO_2. It was plated at an appropriate density (1.0×10^4 cells/well) in 96-well plates and allowed to attach for 24 h. Cells were then treated for 24 h with various concentrations of the compound EL-2 (0.06 – 10 μM). Following this incubation period, the cells tested under irradiation were irradiated. For irradiation of the cells, a LED lamp (Osram, Carnaxide, Portugal) was used with a fluence rate of 23–24 μW/cm^2, which was standardized using a calibrated and controlled light equipment (ILT 1400-A radiometer equipped with SEL033 detector), ensuring that all experiments were performed under the same irradiation conditions and exposure time. Before the experiments, a calibration was performed to ensure the uniformity of the light distribution and that the irradiation parameters (power, duration, distance from the source to the sample) were kept constant in all procedures. Additionally, experiments are performed with non-irradiated groups to validate the consistency of the method.

The cells were irradiated continuously for 30 min. The temperature to which the cells were exposed was carefully monitored to guarantee cell viability. The medium was changed and incubated again for 24 h. After this time, the adherent cells were fixed by adding cold 10 % trichloroacetic acid (TCA; 100 μL) and incubated for 60 min at 4 °C. Plates were then washed with deionized water and subsequently dried; Sulforhodamine B (SRB) solution (0.1 % in 1 % acetic acid, 100 μL) was then added to each plate well and incubated for 30 min at room temperature. Unbound SRB was removed by washing with 1 % acetic acid. Plates were air-dried, the bound SRB was solubilized with 10 mM Tris (200 μL) and the absorbance was measured at 540 nm in ELX800 Microplate Reader (Bio-Tek Instruments, Inc.; Winooski, USA). The results were expressed in compound concentration values that inhibited 50 % of the net cell growth (GI_{50}).

2.5. Development of electrospun membranes

2.5.1. Preparation of polymeric solutions and electrospinning-electrospraying process

For the electrospinning process, solutions of 15 % (w/v) of PCL were prepared in CHF/DMF (80/20), considering the optimized conditions already reported in previous works (Costa et al., 2022; Francavilla et al., 2021; Niknam et al., 2022; Şimşek, 2020; Arrieta et al., 2020). Firstly, PCL pellets were completely dissolved in CHF and stirred for at least 2 h at 35 °C. DMF was then added, and the solution was left under stirring overnight. Different concentrations of EL-2 (2.2×10^{-7}, 4.4×10^{-6}, 2.2×10^{-5}, 2.2×10^{-4}, and 5.5×10^{-4} M) were added to PCL solutions and left under stirring for 2 h in the dark. PCL and PCL+EL-2 solutions were electrospuned in electrospinning NF-103 equipment from MECC Co., Ltd. (Fukuoka, Japan). The optimized conditions able to produce defect-free electrospun membranes were: 1 mL/h of feed rate, 25 kV of voltage, 260 mm of distance between the needle and the collector, and 0.61 mm of needle diameter. A static metallic collector was used to collect the electrospun membranes with 2 h of deposition time.

For the electrospraying process, a solution of 0.5 % (w/v) ChNC was prepared in ethanol. An optimization process of electrospraying method was performed to achieve a stable and continuous cone-jet, and consequently, a homogeneous distribution of ChNC (data not shown). This optimization was conducted considering the study of Azimi et al. (Azimi et al., 2020), which reported the electrospraying of chitin nanofibrils onto PHA electrospun membranes as well as the previous work conducted by our research team, which used electrospray to create homogenous coatings with nanomaterials (Araújo et al., 2024). The ChNC solution was left under stirring for 2 h and put on ultrasound for 30 min. The electrospraying of ChNC dispersion was performed on the developed PCL and PCL+EL-2 membranes for 30 min using 2 mL/h, 20 kV, 100 mm, and 0.41 mm of feed rate, voltage, needle-collector distance, and needle diameter, respectively. All the developed electrospun membranes containing the EL-2 were performed in the dark to prevent degradation. A schematic diagram of the experimental procedure to develop PCL+EL-2/ChNC using electrospinning and electrospraying processes is described in electronic support information (ESI, Fig. S2).

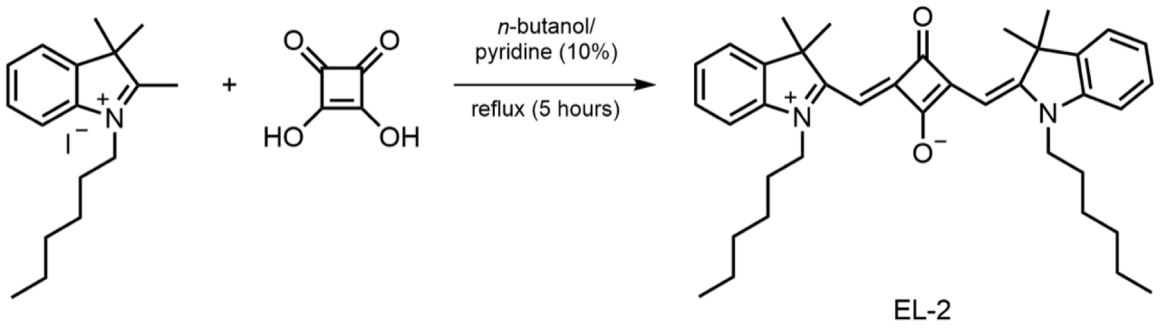

Fig. 1. Synthesis and chemical structure of squaraine EL-2.

2.6. Characterization of ChNC dispersion, polymeric solutions and electrospun membranes

2.6.1. Water contact angle (WCA)

The hydrophobic/hydrophilic character of the developed electrospun membranes was determined using a Contact Angle System (dataphysics) attached to a high-resolution camera. A volume of 5 μL distilled water was deposited onto the sample's surface and the contact angle was measured through the drop shape analysis. Each sample was measured in 10 different places, and the values of mean and standard deviations were calculated.

2.6.2. Field emission scanning electron microscopy (FESEM)

The morphology of the developed electrospun membranes and the presence and distribution of ChNC all over the fibers were evaluated by FESEM, using NOVA 200 Nano SEM, FEI Company (Hillsboro, OR, USA). The samples were coated with a very thin film (20 nm) of Gold-Palladium (Au-Pd) (80–20 wt %), using a high-resolution sputter coater, 208 HR Cressington Company (Watford, UK), coupled to an MTM-20 Cressington High-Resolution Thickness Controller. Secondary electron images, e.g., topographic images, were performed at acceleration voltage of 10 kV. The average diameters of the fibers and the ChNC deposited onto the membranes were calculated in 100 different locations of each sample using *Image J* software. The diameter distribution was assessed as a frequency of the fiber/ChNC diameters.

2.6.3. Attenuated total reflectance-fourier transform infrared spectroscopy (ATR-FTIR)

The chemical composition of the electrospun membranes was evaluated by ATR-FTIR analysis using an IRAffinity-S1, SHIMADZU equipment (Kyoto, Japan). Each spectrum was acquired in transmittance mode using a diamond ATR crystal cell, by accumulation of 45 scanning cycles and with a resolution of 4 cm^{-1}, in the range between 400 and 4000 cm^{-1}.

2.6.4. UV–Visible absorption and fluorescence spectroscopy

The absorption spectrum of EL-2 in DMF was recorded in a Spectrophotometer UV-2600 Shimadzu with the ISR_2600 Plus detector, in the 300 to 800 nm wavelength range. The fluorescence emission spectrum of EL-2 in DMF, as well as PCL+EL-2 electrospun membranes, were acquired in the wavelength range of 300 to 800 nm using a FLEX spectrometer coupled to an LED light source with an excitation wavelength of 525 nm.

2.6.5. Ground state diffuse reflectance (GSDR)

GSDR analysis was performed using a Spectrophotometer UV-2600 Shimadzu with the ISR_2600 Plus detector. The equipment was calibrated using barium sulphate as blank (full reflectance). The reflectance spectra of the developed electrospun membranes were recorded in the wavelength range of 300 to 800 nm. The remission function F(R) was calculated accordingly with the Kubelka-Munk equation:

$$F(R) = \frac{(1-R)^2}{2\,x\,R} = \frac{K}{S} \quad (1)$$

where K is the absorption coefficient, S is the dispersion coefficient and R is the reflectance.

2.6.6. Confocal laser scanning microscopy (CLSM)

CLSM analysis was performed in an Olympus FLUOVIEW FV1000 confocal laser scanning microscope. Electrospun membranes were collected for 3–5 min in a glass coverslip to enable uniform distribution of fibers for image acquisition. The excitation and detection wavelengths were at 559 nm and 575–675 nm, respectively.

2.7. In vitro cytotoxicity of electrospun membranes on HeLa cells

To evaluate the cytotoxicity of each electrospun membrane, a section (1 cm × 1 cm) was used according to the procedure described in section 2.4. However, in this case, the cells were placed in the well and after 1 hour the membranes were added, followed by an incubation period of 24 h. Subsequently, the membranes were removed before cell irradiation (described in section 2.4). The results were expressed as the percentage of inhibition of each membrane in the dark and under light irradiation.

2.8. Statistical analysis

Statistical analysis was performed using a GraphPad prism (version 8.0). Two-way ANOVA test was conducted to evaluate the differences between the cytotoxic effect of the samples under dark and light conditions. Data are presented by mean SD. Statistical significance was considered if $p < 0.0001$.

3. Results and discussion

An innovative strategy was followed in this work by combining fiber formation technique by electrospinning with surface modification by electrospraying, creating non-woven fibrous substrates for cancer PDT applications using a single unit setup. Hence, this work aimed to develop ChNC-coated PCL/EL-2 fibrous platforms by electrospinning-electrospraying method to act as localized implants for photodynamic cancer treatment. As displayed in the schematic representation of Fig. 2, PCL+EL-2 microfibers were produced by electrospinning, followed by their coating with ChNC *via* electrospraying.

3.1. Development and characterization of electrospun ChNC-coated PCL membranes

Extracted chitin nanocrystals (ChNC) are single rod-like particles in suspension, with average length and diameter of 504 ± 158 nm and 27.3 ± 5.99 nm, respectively, and positively charged (ζ-potential *ca.* + 60 mV) (Fig. 3a). PCL filamentous membranes were produced by electrospinning. The polyester nature of PCL imparts these membranes a hydrophobic character, which decreases its biocompatibility and overall biointeractions that are required for the DDS used in photodynamic cancer therapy (Arabi et al., 2013; Ehtesabi & Massah, 2021; Niemczyk-Soczynska et al., 2020; Qin et al., 2021). Surface hydrophilicity of electrospun membranes plays a key role in cell-material interaction (Homaeigohar & Boccaccini, 2022). Water contact angle of pure PCL membranes was *ca.* 140°, bearing super hydrophobicity (Fig. 3b). This is a combined effect of chemistry and morphological features, which increase the WCA due to roughness following the phenomenon described by Cassie and Baxter. To improve the hydrophilicity, and overall biocompatibility and bioactivity of PCL membranes, they were coated with ChNC using electrospray. The WCA of ChNC-coated PCL membranes decreased to 74°, moving from near superhydrophobic to a hydrophilic material. This drastic decrease in contact angle values can be due to the presence of hydrophilic functional groups in ChNC, such as hydroxyl and amide groups (Kim et al., 2012). Goetz et al. reported similar results by converting highly hydrophobic cellulose acetate electrospun microfibers into superhydrophilic upon surface functionalization with ChNC, with the primary contributing factor being the chemical composition of ChNC (Goetz et al., 2016). This result is consistent with previously reported data concerning the production of core-shell electrospun nanofibers, composed of poly(lactic acid) (PLA) as the core and polyacrylonitrile/ChNC as the shell, which also exhibited superhydrophilicity in contrast to hydrophobic PLA core. This finding confirms that ChNC addition contributed to creating a more hydrophilic and less negatively charged surface (Jalvo et al., 2017). These studies

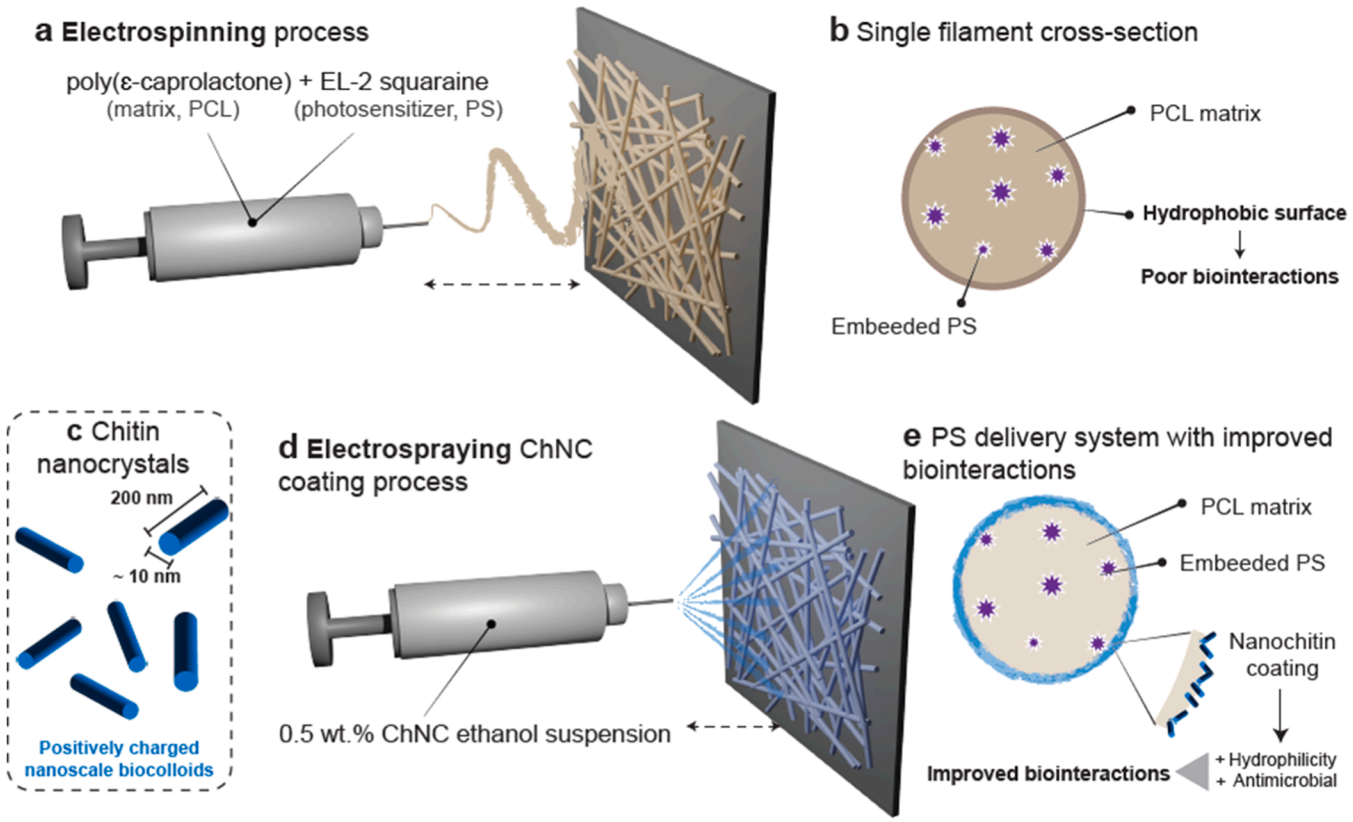

Fig. 2. Overall process of preparing a drug delivery system of a photosensitizer for photodynamic therapy. (a) Electrospinning process of PCL as a matrix and EL-2 squaraine as a photosensitizer. The process yields a (b) PCL filamentous membrane carrying the encapsulated PS. The surface of the single filaments is hydrophobic and displays poor wettability and bio interactions. (c) Chitin nanocrystals are used to coat the membranes via (d) electrospray to yield PCL+EL-2 membranes with a (e) nanochitins coating that is more hydrophilic and antimicrobial.

also showed that ChNC-based electrospun membranes were more resistant to bacterial colonization and biofilm formation, which is a valuable feature for implantable DDS. To the best of the author's knowledge, this is the first study reporting the electrospraying of ChNC. Nevertheless, a few studies have explored the electrospraying of chitin nanofibrils, showing their uniform and successful deposition onto different substrates along with bioactivity (Azimi et al., 2020; Azimi et al., 2021). For instance, Azimi et al. modified the surface of poly-hydroxyalkanoate electrospun membranes *via* electrospraying using chitin nanofibrils, resulting in the improvement of the indirect antimicrobial and anti-inflammatory activity of the electrospun fiber meshes (Azimi et al., 2020).

Randomly aligned PCL microfibers were developed by electrospinning with no defects. Uniform fibers with average diameters of 1.8 μm were produced (Fig. 3 c1). The macroscale morphology of the ChNC-coated PCL membrane remained the same, while the morphology of each individual microfiber displays a much rougher surface due to the coating of single and aggregated ChNCs (Fig. 3 c2). Although ChNC are single rod-like particles in suspension, the scanning electron microscope images in Fig. 3 c2 show that small assemblies of ChNC are visible in the coated layer, which was also corroborated by the diameter distribution histogram, showing higher average diameters compared to single nanocrystals. Under acidic conditions (e.g., pH 3), amino groups on the ChNC surface are protonated, and the cationic charge density on the surface of the crystals increases, thereby enhancing the electrostatic repulsion between them, and consequently, promoting their dispersion. Increasing the pH, even maintaining acid conditions (e.g., pH = 6) may cause less protonation of amino groups, which reduces the electrostatic repulsion between the crystals (Bai et al., 2022; Yang et al., 2020). The addition of ChNC acidic dispersion into ethanol led to an overall pH increase from 3 to 4, which may result in a decrease in cationic charge density, thereby promoting some agglomeration of the nanocrystals. Moreover, the electrospray process may have induced evaporation induced self-assembly of ChNC into supracolloids prior to their deposition onto the PCL microfibers.

ATR-FTIR analysis further confirmed the successful coating of fibrous membranes with ChNC (Fig. 3d). PCL spectrum shows the typical bands of this polymer: 2941 cm^{-1} (asymmetric CH_2 stretching), 2864 cm^{-1} (symmetric CH_2 stretching), 1724 cm^{-1} (carbonyl (C = O) stretching), 1468 cm^{-1} (C—C bending), 1294 cm^{-1} (C—O and C—C stretching in the crystalline phase), 1240 cm^{-1} (asymmetric C–O–C stretching), 1167 cm^{-1} (symmetric C–O–C stretching) and 1107 cm^{-1} (C—O and C—C stretching in the amorphous phase) (Costa et al., 2022). New bands appeared in the spectrum of ChNC-coated PCL membranes, including those at 3441 cm^{-1}, which correspond to O—H stretching, and the ones at 3264 and 3107 cm^{-1} that are attributed to N—H stretching of the amide and amine groups, respectively (Azimi et al., 2020; Pereira et al., 2020). The characteristic amide bands are also detected at 1659 and 1558 cm^{-1}, which are attributed to the stretching of C = O in the amide I, and the overlapping of the C—N stretching and N—H bending in the amide II, respectively (Zhong et al., 2020). These findings corroborate the presence of ChNC on the surface of PCL microfibers.

3.2. Assessment of the cytotoxic of squaraine EL-2 in HeLa cells and its incorporation in PCL electrospun membranes

The synthetic methodologies to produce the squaraine EL-2, as well as the full structural characterization of the dye, were recently reported by some of us (Lima et al., 2019). EL-2 squaraine dye demonstrated properties inherent to those of an ideal photosensitizer, such as the ability to produce singlet oxygen, unquestionable light stability, and, for some cell lines under study, very promising photodynamic activity.

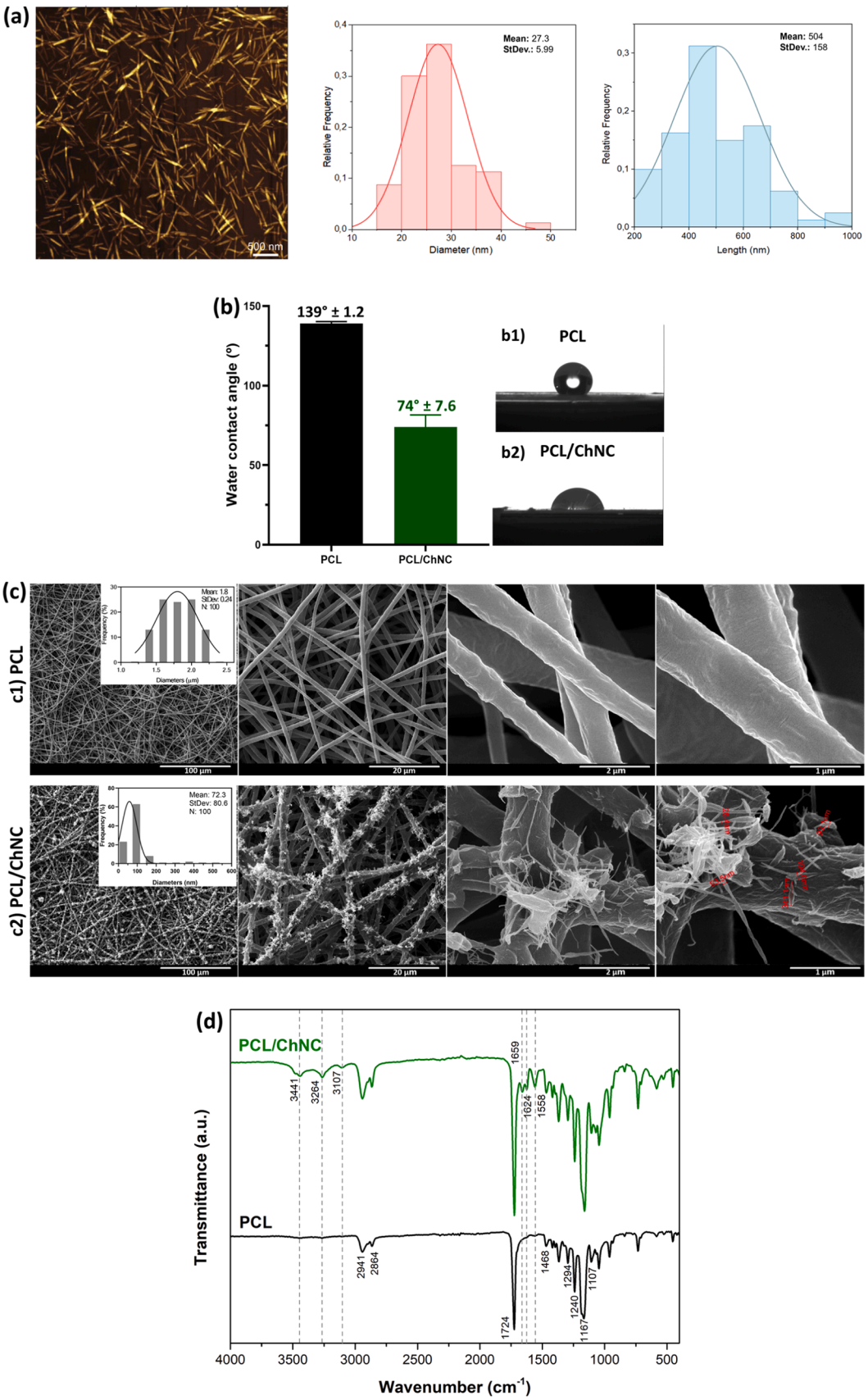

Fig. 3. Chemical and structural properties of pure and ChNC-coated PCL membranes. (a) Atomic Force Microscopy (AFM) image of ChNC dispersion and distribution histograms of diameter and length of the extracted ChNC. (b) Average Water Contact Angle (WCA) and (b1-b2) images of droplet cast on the pure and coated membranes. (c) Field-Emission Scanning Electron Microscopy (FESEM) images of (c1) pure and (c2) ChNC-coated PCL membranes and their respective diameter distribution histograms, and (d) ATR-FTIR spectra of PCL and ChNC-coated PCL electrospun membranes.

Moreover, to verify its tumor selectivity, its cytotoxicity was also evaluated against non-tumor cells, including normal human dermal fibroblasts (NHDF), revealing a selective effect in this cell line, with no marked observed cytotoxic effects, either in the presence or absence of irradiation exposure (Lima et al., 2019). Thus, it would be expected that the encapsulation of EL-2 within fibrous membranes would result in equal or less pronounced effects on the cell viability of this fibroblast cell line, without compromising the tumor selectivity observed for this dye. This selective photocytotoxic effect of EL-2 aligned with the intrinsic selectivity of PDT, which derives from the localized irradiation of the target area, can improve the therapeutic efficacy while reducing the side effects on healthy tissues (Costa et al., 2022). In this work, to evaluate the *in vitro* photodynamic effect of this molecule against HeLa cervical carcinoma cells, its cytotoxicity in the dark and under irradiation was determined. The results are expressed in half-maximal growth inhibitory values (GI_{50}; Fig. 4a). Ideally, a PS must exhibit absence or minimal toxicity in the dark and high toxicity under irradiation (Lima & Reis, 2023). Results from Fig. 4a demonstrate that EL-2 can inhibit 50 % of HeLa cell growth at a concentration of approximately 4.38 μM. Nevertheless, when these molecules are irradiated, the GI_{50} values considerably decrease to 0.22 μM, showing that a lower concentration of EL-2 is required to inhibit 50 % of cancer cell growth upon irradiation. These findings confirm the phototherapeutic potential of EL-2 since this squaraine displayed about 20 times more photocytotoxicity compared to the dark condition.

The promising photodynamic activity of EL-2 dye is not surprising, given that, for Caco-2, MCF-7, and PC-3 cell lines (colorectal adenocarcinoma, breast, and prostate cancer cell lines, respectively), significantly lower half-maximal inhibitory concentration values were reported by Lima et al. under irradiated conditions (IC_{50} between 1.1 and 3.3 μM treated for 14 min) compared to dark conditions ($IC_{50} > 10$ μM). However, effectively, under the conditions tested in the present study, the photocytotoxicity of the dye proved to be more interesting, maintaining a good safety margin between the concentration at which it is effectively phototoxic and harmless in the dark, suggesting its potential interest in a therapeutic approach to cervical carcinoma. The direct comparison with other analogous molecules is difficult, as, according to our experience, the zwitterionic unsubstituted squaraines generally face solubility issues. An example of this is the benz[*e*]indole-based analog recently published by some of us, which did not show biological interest due to its easy aggregation and precipitation in aqueous solutions (Lima & Reis, 2022). However, other derivatives of indolenine, with variations in *N*-alkyl chains, have also shown promise in their potential phototherapeutic application, even compared to aminosquaraine or thiosquaraines (Fernandes et al., 2020; Lima et al., 2020), demonstrating that unsubstituted squaraines can be particularly advantageous for PDT applications. The normalized absorption spectrum of EL-2 in DMF (Fig. 4b) showed that this compound exhibits a strong absorption where the light penetration in living tissues is higher in this region, which is advantageous for PDT applications. EL-2 presented a maximum absorption intensity at 642 nm and a characteristic hypsochromic shoulder typical for polymethine dyes (Bordignon et al., 2023). EL-2 could also emit fluorescence, with a maximum emission detected at 676 nm ($\lambda_{exc.} = 525$ nm).

After confirming the photodynamic effect of EL-2 dye on HeLa cells, different EL-2 concentrations were incorporated into the PCL solutions prior to electrospinning. Accounting for the cytotoxicity values, we introduced 2.2×10^{-7}, 4.4×10^{-6}, 2.2×10^{-5}, 2.2×10^{-4}, and 5.5×10^{-4} M of EL-2 into PCL to correspond to 1 ×, 20 ×, 100 ×, 1000 ×, and 2500 × of the measured GI_{50} value under light irradiation. Figs. 4c–e shows the Ground State Diffuse Reflectance (GSDR) and fluorescence spectra of PCL+EL-2 membranes as well as Confocal Laser Scanning Microscopy (CLSM) images of the developed membranes.

The remission function was calculated according to the Kubelka-Munk equation (Eq. (1)), and the recorded PCL+EL-2 membranes spectra are presented in Fig. 4c. PCL membranes did not present any absorption band. On the other hand, PCL+EL-2 membranes bearing different squaraine concentrations exhibited the typical absorption bands of the compound, confirming the successful incorporation of EL-2 in the electrospun microfibers. Even with the lowest EL-2 concentration (2.2×10^{-7} M), a tenue absorption band was observed, evidencing its presence within PCL microfibers. The maximum absorption intensity was detected at *ca.* 640 nm for all EL-2 concentrations. Moreover, as the EL-2 increases, the intensity of the main band also increases as well as the intensity of the shoulder around 594 nm.

The fluorescence spectra of the developed electrospun membranes were also recorded (Fig. 4d). PCL+2.2×10^{-7} M EL-2 membranes, did not present any fluorescence band. On the other hand, when using 4.4×10^{-6}, 2.2×10^{-5}, 2.2×10^{-4}, and 5.5×10^{-4} M of EL-2, the fluorescence band was visible, with a maximum emission at 653, 658, 679, and 685 nm, respectively. As the loading of the dye in the membranes increases, a bathochromic shift is observed. One possible contributor to this phenomenon is dye aggregation within the polymer matrix. Squaraine dyes are known to exhibit strong aggregation tendencies, and as reported by Vieira Ferreira et al. (Ferreira et al., 2016; Ferreira et al., 2013; Ferreira et al., 1996; Oliveira et al., 1996), such aggregation leads to characteristic spectral changes, particularly in absorption, depending on the type of aggregate formed. Although absorption spectra provide more definitive evidence of aggregation, changes in emission behavior can also be indicative of such interactions, particularly when accompanied by quenching or shifts in peak position. CLSM images indicated the presence and distribution of the dye within microfibers. Membranes with the lowest, intermediate, and highest concentrations of EL-2 (2.2×10^{-7}, 2.2×10^{-5} and 5.5×10^{-4} M) were excited at 559 nm and the emission fluorescence was detected at 575–675 nm. Brightfield visualization revealed the presence of PCL microfibers, however, when these fibers were excited at 559 nm, a black image appeared, demonstrating that these membranes did not exhibit any fluorescent. Likewise, no fluorescence was detected with the introduction of the lowest EL-2 concentration, which corroborates the fluorescence spectrum recorded for PCL+2.2×10^{-7} M EL-2 membranes. On the contrary, PCL membranes loaded with 2.2×10^{-5} and 5.5×10^{-4} M EL-2 showed fluorescence in the red region. The good dispersion of the dye molecules within the fibers was confirmed by the even distribution of the fluorescence along the microfibers, with only very few discontinuities in the red signal detected. PCL+5.5×10^{-4} M EL-2 membrane displayed a more intense fluorescence, resulting from the higher EL-2 concentration incorporated. The surface of PCL membranes remained hydrophobic after the encapsulation of distinct EL-2 concentrations, confirmed by the very similar WCA values (Fig. 4f). Overall, these techniques demonstrated the successful incorporation and dispersion of EL-2 dye onto electrospun fibrous membranes. Furthermore, EL-2 dyes were able to preserve their fluorescence properties after their incorporation onto substrates, which is of great importance to achieve theranostic systems, which combine both cancer diagnosis and therapy (Sarbadhikary et al., 2021).

3.3. Coating of PCL+EL-2 electrospun membranes with ChNC by electrospraying

Once the squaraine dye was properly incorporated into the microfibers, ChNC were deposited onto PCL+EL-2 membranes *via* electrospraying technique using the optimized parameters previously discussed. FESEM images of PCL+EL-2 membranes coated with 0.5 % ChNC (Fig. 5) show that the morphology of the coated PCL+EL-2 microfibers remained practically unchanged, displaying defect-free microfibers regardless of the amount of EL-2 introduced. The deposition of ChNC was also successfully performed, exhibiting a morphology similar to those coated on pure PCL membranes (Fig. 3 c2). FESEM images of PCL membranes containing the other EL-2 concentrations were provided in the electronic support information (ESI, Fig. S3).

(a)

CONDITIONS	GI_{50} (μM)
Dark	4.38 ± 0.38
Light irradiation	0.22 ± 0.02

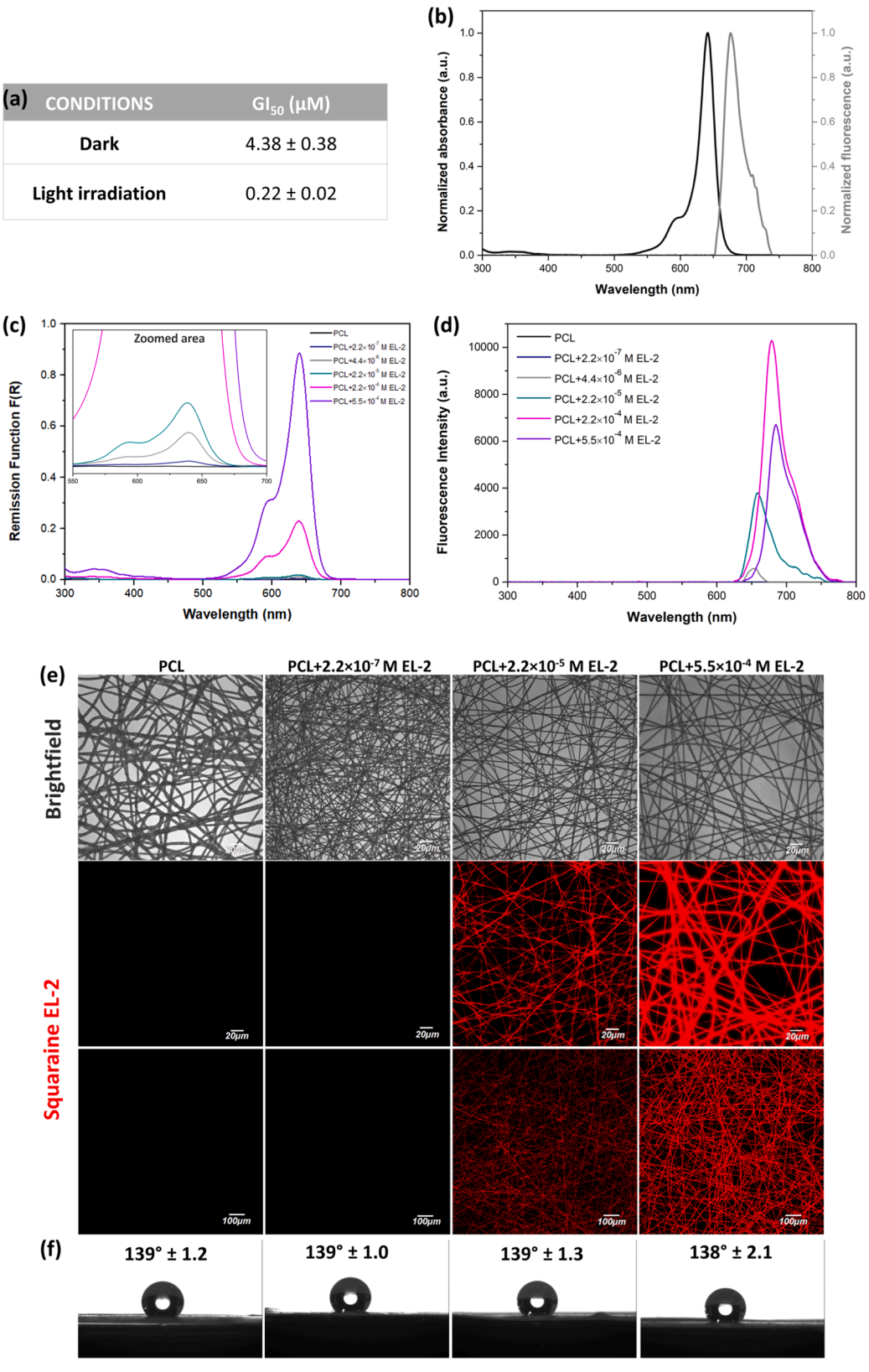

Fig. 4. Cytotoxicity of EL-2 squaraine dye and absorption and fluorescence analysis of electrospun PCL+EL-2 membranes. (a) Cytotoxicity (GI_{50} values, μM; mean ± standard deviation) of EL-2 in its free form in the dark and under irradiation conditions against HeLa cervical carcinoma cells. (b) Normalized spectra of absorption and fluorescence emission of squaraine dye EL-2 in DMF. The fluorescence emission spectrum was obtained with an excitation wavelength of 525 nm. (c) Ground State Diffuse Reflectance (GSDR) and (d) fluorescence emission ($\lambda_{exc.} = 525$ nm) spectra of PCL and PCL+EL-2 (2.2×10^{-7}, 4.4×10^{-6}, 2.2×10^{-5}, 2.2×10^{-4}, and 5.5×10^{-4} M) electrospun membranes. (e) Confocal Laser Scanning Microscopy (CLSM) of PCL and PCL+EL-2 (2.2×10^{-7}, 2.2×10^{-5} and 5.5×10^{-4} M) electrospun membranes excited at 559 nm and detected at 575–675 nm. (f) Average Water Contact Angle (WCA) and images of droplet cast on the PCL and PCL+EL-2 (2.2×10^{-7}, 2.2×10^{-5} and 5.5×10^{-4} M) electrospun membranes.

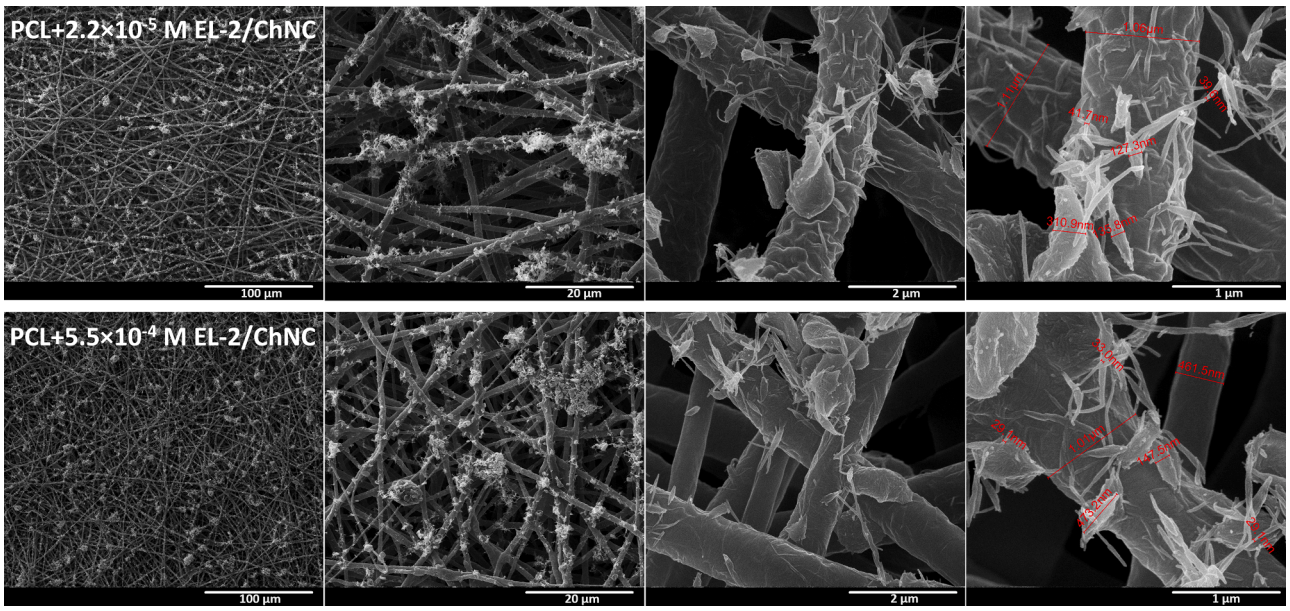

Fig. 5. Field Emission Scanning Electron Microscopy (FESEM) images of PCL+2.2 × 10^{-5} M EL-2 and PCL+5.5 × 10^{-4} M EL-2 electrospun membranes, which were coated with 0.5 % ChNC in ethanol *via* electrospraying.

3.4. Phototherapeutic potential of electrospun membrane-based implants

As previous reported (Lima et al., 2019), following 24 h of incubation of EL-2 with tumor cells, this squaraine permeated the cytoplasmic membrane and accumulated in certain cytoplasmic structures, thereby confirming its intracellular internalization after 24 h. Therefore, to evaluate the photodynamic action of EL-2 after being encapsulated into fibrous substrates, the developed membranes were put in contact with HeLa cells for 24 h, and then removed before cell irradiation. The inhibition percentage of each membrane on HeLa cells in dark and light conditions was calculated (Fig. 6), reflecting the ability of the fibrous system to prevent cell proliferation, being higher values indicative of less growth of cancer cells. PCL/ChNC exhibited minimal toxicity in both conditions, demonstrating a percentage of inhibition of 2.76 % in the dark and 3.78 % in the light (Panda et al., 2024). This result could be related to the presence of some residual solvents used to produce the electrospun membranes, such as chloroform and DMF. The slight difference between both conditions (1.02 %) suggests that there is no specific toxicity upon irradiation, proving that PCL/ChNC are not by themselves suitable as PDT agents, while reinforces their biosafety for biomedical applications (Panda et al., 2024).

The addition of different EL-2 concentrations in the fibrous mats promoted an increase of inhibition values both in the dark and light conditions, which was shown to be proportional to the squaraine concentration. However, the cancer cell proliferation inhibition was always higher under light irradiation than to darkness, confirming the specific activation by light of the squaraine-loaded membranes. These results validate that EL-2 not only exhibits a strong photodynamic effect in solution (Fig. 4a), but also retains its photoactivity when integrated into fibrous substrates. Microfibers loaded with 2.2 × 10^{-7} EL-2, which was the lowest amount determined to inhibit 50 % of HeLa cells when used in solution, could inhibit around 20 % of cell proliferation under

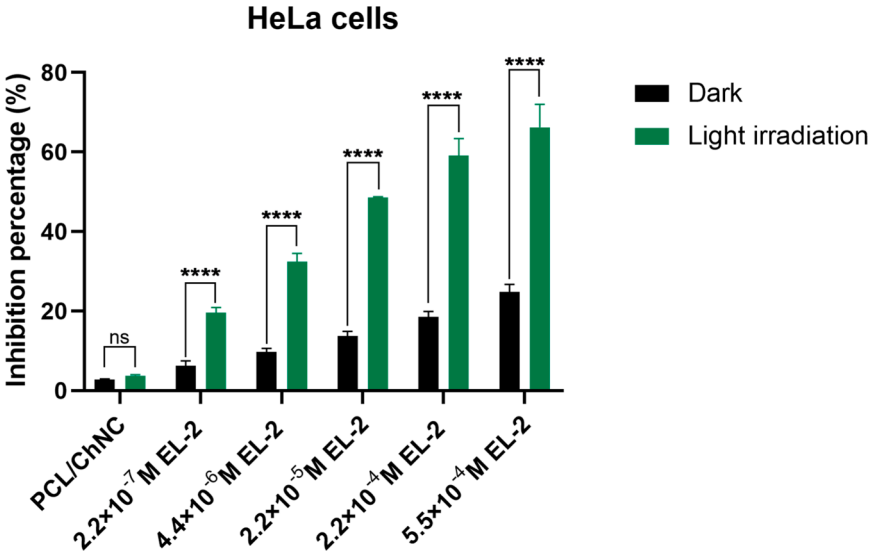

Fig. 6. Photodynamic effect of the developed electrospun membranes. Inhibition percentage (% mean ± standard deviation) of PCL/ChNC and PCL+EL-2/ChNC containing different EL-2 concentrations (2.2 × 10^{-7}, 4.4 × 10^{-6}, 2.2 × 10^{-5}, 2.2 × 10^{-4} and 5.5 × 10^{-4} M) electrospun membranes on the proliferation of HeLa cells in dark and light-exposed experimental conditions. ns: not significant; ****: $p < 0.0001$.

irradiation. Moreover, the difference between dark and light conditions was statistically significant, thereby confirming the specificity of the loaded EL-2 to light.

Increasing the concentration of EL-2 in the electrospun microfibers, led to a higher percentage of inhibition both in the dark and light conditions. Nonetheless, the difference between inhibition values in the dark and under irradiation, using membranes containing 4.4×10^{-6}, 2.2×10^{-5}, 2.2×10^{-4} and 5.5×10^{-4} M of the evaluated dye, significantly increased to 22.69, 34.75, 40.62 and 41.47 inhibition proliferation percentages, respectively. The maximum loaded amount of EL-2 inhibited 66.25 % of cell proliferation under irradiation.

The use of HeLa cells shows the potentiality of these fibrous phototherapeutic platforms to treat cervical cancer with light. Moreover, the easy accessibility of the cervix through the vaginal canal allows the non-invasive implantation of these DDS, which enables the direct delivery of the dyes onto or adjacent to tumor tissues (Ghosh et al., 2022).

The combination of PDT as localized therapy with electrospun micro/nanofibers as localized carriers is an emerging area of exploration. A few studies have already established the proof of concept regarding using PS-loaded electrospun membranes as DDS for cancer PDT. For instance, Ma et *al.* showed that poly(l-lactic) acid (PLLA)/polyethylene oxide (PEO) containing 5,10,15,20-tetrakis (4-carboxyphenyl) porphyrin (TCPP) as PS exhibited photodynamic interest against HeLa cells (Ma et al., 2018). Chitosan/PEO nanofibers incorporated with Photosens sulfonated aluminum phthalocyanine were also developed for cancer PDT applications. The research confirmed a PS dose-dependent dark toxicity, being that lower PS concentrations did not affect the cellular metabolism while higher promoted a slight T-47D breast cancer cells metabolic inhibition. On the other hand, at the lower dark harmless concentrations, the light exposure induced a more significant reduction in metabolic activity, highlighting the potential PDT application of PS-loaded electrospun nanofibers (Severyukhina et al., 2016). Recently, our research group developed biodegradable core-shell nanofibers loaded with porphyrin to act as localized DDS for cervical cancer PDT. The developed core-shell fibrous structures exhibited higher cytotoxicity on HeLa cells under light irradiation than in the dark. Additionally, a selective photocytotoxic effect appears to occur in tumor cell lines compared to non-tumor cells (Costa et al., 2024).

However, establishing direct comparisons between the results presented in this study and those reported in the literature remains extremely difficult due to the high variability in the experimental procedures and used materials, that can significantly affect the final performance of the fibrous systems for PDT. These variables include the type and concentration of PS employed, which directly influences the efficiency to generate ROS, and consequently, the photodynamic effect. Furthermore, the composition, morphology and structure of the developed electrospun membranes will also influence the PS-release profile and cell-material interactions. The type of cells used for *in vitro* assays as well as the characteristics of light source and irradiation time also extremely vary between studies, further contributing to the heterogeneity across studies. All these differences make a direct benchmarking analysis challenging while highlight the importance of standardized protocols for evaluating PDT implants. Despite the difficulty in directly comparing results, this study demonstrated that even the lowest EL-2 concentration within PCL membranes resulted in a statistically difference in the inhibition of cell proliferation between dark and light conditions. This tendency became more pronounced with increasing EL-2 concentrations. Additionally, in absence of radiation, the reduction in cell viability was always <30 %, which is the threshold level for cytotoxicity according to International Standard (Lima et al., 2022; Lima et al., 2025; 2009. ISO-10993–5, 2009). Therefore, all these findings demonstrate the potential of these fibrous platforms for cancer PDT.

4. Conclusions

Fibrous phototherapeutic platforms based on biodegradable PCL+EL-2/ChNC microfiber implants for treating cancer using PDT were successfully developed through an electrospinning-electrospraying approach. Considering the advantages of having a balanced hydrophilic surface over a hydrophobic one to foster cell-material interactions, ChNC were used to modify the surface of PCL membranes and potentially impart bioactivity. FESEM and ATR-FTIR techniques confirmed the presence of ChNC on the membrane's surface and their good dispersion along PCL fibers. WCA of PCL membranes changed from 139° to 74° with the addition of ChNC, making the membrane's surface hydrophilic – a desirable property for an implant since it promotes cell adhesion. EL-2 squaraine demonstrated an *in vitro* photodynamic effect against HeLa cells, displaying a GI_{50} value of 4.38 μM in the dark and 0.22 μM when exposed to light, confirming its great potential as a PS agent. Several EL-2 concentrations (2.2×10^{-7}, 4.4×10^{-6}, 2.2×10^{-5}, 2.2×10^{-4} and 5.5×10^{-4} M) were added to PCL polymeric solutions to produce electrospun PCL+EL-2 microfibers. The presence and well distribution of EL-2 within PCL fibers were confirmed by GSDR, fluorescence spectroscopy and CLSM. Moreover, incorporating the squaraine did not change the fibers' morphology. Finally, PCL+EL-2/ChNC membranes exhibited higher inhibition proliferation of HeLa cells under light irradiation compared to dark conditions, achieving maximum inhibition of 66.25 % when exposed to radiation. These fibrous platforms were able not only to carry PS molecules while maintaining their phototherapeutic effect after incorporation into microfibers but also have the potential to act as active agents by mimicking the ECM and promoting cell-material interaction. The total customizability of this technology and its scalability to the industrial level highlights its great potential to produce different DDS that can meet various needs, considering patient-to-patient variabilities. Future work will be conducted to evaluate the bioactivity of the final fibrous systems, particularly their antimicrobial activity, as well as their biodegradability in biological media and the photodynamic effect over time. These studies will provide new insights regarding their potential for *in vivo* applications and eventual clinical translation.

CRediT authorship contribution statement

Sofia M. Costa: Writing – original draft, Methodology, Conceptualization. **Bruno D. Mattos:** . **Ricardo C. Calhelha:** Writing – review & editing, Methodology. **Ya Zhu:** Methodology. **Eurico Lima:** Writing – review & editing, Methodology. **Lucinda V. Reis:** Writing – review & editing. **Orlando J. Rojas:** Writing – review & editing, Validation, Supervision. **Raul Fangueiro:** Writing – review & editing, Validation, Supervision. **Diana P. Ferreira:** Writing – review & editing, Validation, Supervision, Conceptualization.

Declaration of competing interest

The authors declare that they have no known competing financial interests or personal relationships that could have appeared to influence the work reported in this paper.

Acknowledgments

This work was funded by the European Regional Development Fund through the Operational Competitiveness Program and the National Foundation for Science and Technology of Portugal (FCT) under the projects UID/CTM/00264/2020 of Centre for Textile Science and Technology (2C2T) on its components Base (https://doi.org/10.54499/UIDB/00264/2020) and programmatic (https://doi.org/10.54499/UIDP/00264/2020). The authors are also thankful to the projects UID/QUI/UI0616/2019 – Chemistry Centre of Vila Real, funded by National Founds through FCT/MCTES - Fundação para a Ciência e a Tecnologia. Sofia M. Costa and Eurico Lima are thankful for the FCT PhD Scholarships SFRH/BD/147517/2019 and SFRH/BD/147645/2019, respectively. The authors are also grateful to the Foundation for Science

and Technology (FCT, Portugal) for financial support through national funds FCT/MCTES (PIDDAC) to CIMO (UIDB/00690/2020 and UIDP/00690/2020) and SusTEC (LA/P/0007/2020); the contract of RC Calhelha through the institutional scientific employment program-contract (CEEC-INST; DOI:10.54499/CEECINST/00016/2018/CP1505/CT0009).

Supplementary materials

Supplementary material associated with this article can be found, in the online version, at doi:10.1016/j.carpta.2025.100895.

Data availability

Data will be made available on request.

References

2009. ISO-10993-5. (2009). International Standard is, biological evaluation of medical devices. Part 5. *Tests for in Vitro Cytotoxicity*. third ed., International Standard Is, Biological Evaluation of Medical Devices. Part 5. Tests for in Vitro Cytotoxicity, third ed.ISO-10993-5., (n.d.).

Ahmad Wsoo, M., Izwan Abd Razak, S., Shahir, S., Ahmed Abdullah Al-Moalemi, H., Rafiq Abdul Kadir, M., & Hasraf Mat Nayan, N. (2021). Development of prolonged drug delivery system using electrospun cellulose acetate/polycaprolactone nanofibers: Future subcutaneous implantation. *Polymers for Advanced Technologies, 32*, 3664–3678. https://doi.org/10.1002/pat.5375

Algorri, J. F., Ochoa, M., Roldán-Varona, P., Rodríguez-Cobo, L., & López-Higuera, J. M. (2021). Light technology for efficient and effective photodynamic therapy: A critical review. *Cancers*, 13. https://doi.org/10.3390/cancers13143484

Al-Jamal, A. N., Al-Hussainy, A. F., Mohammed, B. A., Abbas, H. H., Kadhim, I. M., Ward, Z. H., Mahapatra, D. K., Joseph, T. M., kianfar, E., & Thomas, S. (2025). Photodynamic Therapy (PDT) in drug delivery: Nano-innovations enhancing treatment outcomes. *Health Sciences Review, 14*, Article 100218. https://doi.org/10.1016/j.hsr.2025.100218

Alves, D., Araújo, J. C., Fangueiro, R., & Ferreira, D. P. (2023). Localized therapeutic approaches based on micro/nanofibers for cancer treatment. *Molecules*, 28. https://doi.org/10.3390/molecules28073053

Arabi, A., Boggs, E., Patel, M., Zwiesler-Vollick, J., Maerz, T., Baker, K., Tuck, S., Corey, J., & Li, Y. (2013). Surface modification of electrospun polycaprolactone fibers and effect on cell proliferation. *Surface Innovations, 2*. https://doi.org/10.1680/si.13.00018

Araújo, J. C., Silva, P. M., Cerqueira, M. A., Teixeira, P., Tira-Picos, V., Neto, P., Soares, O. S. G. P., Graça, C. L., Fangueiro, R., & Ferreira, D. P. (2024). Protective fibrous structures based on cellulose fibers functionalized with metal oxide nanoparticles by electrospinning and electrospray deposition. *International Journal of Biological Macromolecules, 282*, Article 137218. https://doi.org/10.1016/j.ijbiomac.2024.137218

Arrieta, M. P., Leonés Gil, A., Yusef, M., Kenny, J. M., & Peponi, L. (2020). Electrospinning of PCL-based blends: Processing optimization for their scalable production. *Materials*, 13. https://doi.org/10.3390/ma13173853

Azimi, B., Ricci, C., Fusco, A., Zavagna, L., Linari, S., Donnarumma, G., Hadrich, A., Cinelli, P., Coltelli, M.-B., Danti, S., & Lazzeri, A. (2021). Electrosprayed shrimp and mushroom nanochitins on cellulose tissue for skin contact application. *Molecules, 26*. https://doi.org/10.3390/molecules26144374

Azimi, B., Thomas, L., Fusco, A., Kalaoglu-Altan, O. I., Basnett, P., Cinelli, P., De Clerck, K., Roy, I., Donnarumma, G., Coltelli, M.-B., Danti, S., & Lazzeri, A. (2020). Electrosprayed Chitin nanofibril/electrospun polyhydroxyalkanoate Fiber mesh as functional nonwoven for skin application. *Journal of Functional Biomaterials, 11*. https://doi.org/10.3390/jfb11030062

Bai, L., Kämäräinen, T., Xiang, W., Majoinen, J., Seitsonen, J., Grande, R., Huan, S., Liu, L., Fan, Y., & Rojas, O. J. (2020). Chirality from cryo-electron tomograms of nanocrystals obtained by lateral disassembly and surface etching of never-dried chitin. *ACS Nano, 14*, 6921–6930. https://doi.org/10.1021/acsnano.0c01327

Bai, L., Liu, L., Esquivel, M., Tardy, B. L., Huan, S., Niu, X., Liu, S., Yang, G., Fan, Y., & Rojas, O. J. (2022). Nanochitin: Chemistry, structure, assembly, and applications. *Chemical Reviews, 122*, 11604–11674. https://doi.org/10.1021/acs.chemrev.2c00125

Bastiancich, C., Danhier, P., Préat, V., & Danhier, F. (2016). Anticancer drug-loaded hydrogels as drug delivery systems for the local treatment of glioblastoma. *Journal of Controlled Release, 243*, 29–42. https://doi.org/10.1016/j.jconrel.2016.09.034

Bordignon, N., Köber, M., Chinigò, G., Pontremoli, C., Sansone, E., Vargas-Nadal, G., Moran Plata, M. J., Fiorio Pla, A., Barbero, N., Morla-Folch, J., & Ventosa, N. (2023). Quatsomes loaded with squaraine dye as an effective photosensitizer for photodynamic therapy. *Pharmaceutics*, 15. https://doi.org/10.3390/pharmaceutics15030902

Cavo, M., Serio, F., Kale, N. R., D'Amone, E., Gigli, G., & del Mercato, L. L. (2020). Electrospun nanofibers in cancer research: From engineering of in vitro 3D cancer models to therapy. *Biomaterials Science, 8*, 4887–4905. https://doi.org/10.1039/D0BM00390E

CeCe, R., Jining, L., Islam, M., Korvink, J. G., & Sharma, B. (2023). An overview of the electrospinning of polymeric nanofibers for biomedical applications related to drug delivery. *Advanced Engineering Materials N/A.* , Article 2301297. https://doi.org/10.1002/adem.202301297

Chng, E. J., Watson, A. B., Suresh, V., Fujiwara, T., Bumgardner, J. D., & Gopalakrishnan, R. (2019). Adhesion of electrosprayed chitosan coatings using silane surface chemistry. *Thin Solid Films, 692*, Article 137454. https://doi.org/10.1016/j.tsf.2019.137454

Costa, S. M., Fangueiro, R., & Ferreira, D. P. (2022a). Drug delivery systems for photodynamic therapy: The potentiality and versatility of electrospun nanofibers. *Macromolecular Bioscience, 22*, Article 2100512. https://doi.org/10.1002/mabi.202100512

Costa, S. M., Lourenço, L. M. O., Calhelha, R. C., Calejo, I., Barrias, C. C., Fangueiro, R., & Ferreira, D. P. (2024). Localized cancer photodynamic therapy approach based on core–shell electrospun nanofibers††electronic supplementary information (ESI) available, 10.1039/d4ma00647j *Materials Advances, 5*, 6489–6500. https://doi.org/10.1039/d4ma00647j.

Costa, S. M., Pacheco, L., Antunes, W., Vieira, R., Bem, N., Teixeira, P., Fangueiro, R., & Ferreira, D. P. (2022b). Antibacterial and biodegradable electrospun filtering membranes for facemasks: An attempt to reduce disposable masks use. *Applied Sciences, 12*. https://doi.org/10.3390/app12010067

Ehtesabi, H., & Massah, F. (2021). Improvement of hydrophilicity and cell attachment of polycaprolactone scaffolds using green synthesized carbon dots. *Materials Today Sustainability, 13*, Article 100075. https://doi.org/10.1016/j.mtsust.2021.100075

Fernandes, T. C. D., Lima, E., Boto, R. E., Ferreira, D., Fernandes, J. R., Almeida, P., Ferreira, L. F. V, Silva, A. M., & Reis, L. V. (2020). In vitro phototherapeutic effects of indolenine-based mono- and dithiosquaraine cyanine dyes against caco-2 and HepG2 human cancer cell lines. *Photodiagnosis and Photodynamic Therapy, 31*, Article 101844. https://doi.org/10.1016/j.pdpdt.2020.101844

Ferreira, D. P., Conceicao, D. S., Calhelha, R. C., Sousa, T., Socoteanu, R., Ferreira, I. C. F. R., & Vieira Ferreira, L. F. (2016). Porphyrin dye into biopolymeric chitosan films for localized photodynamic therapy of cancer. *Carbohydrate Polymers, 151*, 160–171. https://doi.org/10.1016/j.carbpol.2016.05.060

Ferreira, D. P., Conceição, D. S., Fernandes, F., Sousa, T., Calhelha, R. C., Ferreira, I. C. F. R., … Vieira Ferreira, L. F. (2016). Characterization of a Squaraine/chitosan system for photodynamic therapy of cancer. *The Journal of Physical Chemistry B, 120*, 1212–1220. https://doi.org/10.1021/acs.jpcb.5b11604

Ferreira, D. P., Conceicao, D. S., Ferreira, V. R. A., Graca, V. C., Santos, P. F., & Vieira Ferreira, L. F. (2013). Photochemical properties of squarylium cyanine dyes. *Photochemical & photobiological sciences : Official journal of the european photochemistry association and the european society for photobiology, 12*, 1948–1959. https://doi.org/10.1039/c3pp50132a

Ferreira, L. F. V., Oliveira, A. S., Wilkinson, F., & Worrall, D. (1996). Photophysics of cyanine dyes on surfaces. A new emission from aggregates of 2{,}2′-cyanines adsorbed onto microcrystalline cellulose. *Journal of the Chemical Society, Faraday Transactions, 92*, 1217–1225. https://doi.org/10.1039/FT9969201217

Francavilla, P., Ferreira, D. P., Araújo, J. C., & Fangueiro, R. (2021). Smart fibrous structures produced by electrospinning using the combined effect of PCL/graphene nanoplatelets. *Applied Sciences, 11*. https://doi.org/10.3390/app11031124

Francis, L., & Hilal, N. (2022). Electrosprayed CNTs on electrospun PVDF-Co-HFP membrane for robust membrane distillation. *Nanomater*, 12. https://doi.org/10.3390/nano12234331

Friães, S., Lima, E., Boto, R. E., Ferreira, D., Fernandes, J. R., Ferreira, L. F. V, Silva, A. M., & Reis, L. V. (2019). Photophysicochemical properties and In vitro phototherapeutic effects of iodoquinoline- and benzothiazole-derived unsymmetrical squaraine cyanine dyes. *Applied Sciences, 9*. https://doi.org/10.3390/app9245414

Fu, Y., Li, X., Ren, Z., Mao, C., & Han, G. (2018). Multifunctional electrospun nanofibers for enhancing localized cancer treatment. *Small, 14*, Article 1801183. https://doi.org/10.1002/smll.201801183

Gaydhane, M. K., Sharma, C. S., & Majumdar, S. (2023). Electrospun nanofibres in drug delivery: Advances in controlled release strategies. *RSC Advances, 13*, 7312–7328. https://doi.org/10.1039/D2RA06023J

Gazaille, C., Sicot, M., Saulnier, P., Eyer, J., & Bastiat, G. (2021). Local delivery and glioblastoma: Why not combining sustained release and targeting? *Frontiers in Medical Technology, 3*. https://doi.org/10.3389/fmedt.2021.791596

Ghosal, K., Chandra, A., P, G., S, S., Roy, S., Agatemor, C., Thomas, S., & Provaznik, I. (2018). Electrospinning over solvent casting: Tuning of mechanical properties of membranes. *Scientific Reports, 8*, 5058. https://doi.org/10.1038/s41598-018-23378-3

Ghosh, S., Jayaram, P., Kabekkodu, S. P., & Satyamoorthy, K. (2022). Targeted drug delivery in cervical cancer: Current perspectives. *European Journal of Pharmacology, 917*, Article 174751. https://doi.org/10.1016/j.ejphar.2022.174751

Goetz, L. A., Jalvo, B., Rosal, R., & Mathew, A. P. (2016). Superhydrophilic anti-fouling electrospun cellulose acetate membranes coated with chitin nanocrystals for water filtration. *Journal of Membrane Science, 510*, 238–248. https://doi.org/10.1016/j.memsci.2016.02.069

Goonoo, N., Bhaw-Luximon, A., & Jhurry, D. (2014). Drug loading and release from electrospun biodegradable nanofibers. *Journal of Biomedical Nanotechnology, 10*, 2173–2199. https://doi.org/10.1166/jbn.2014.1885

Hoare, T. R., & Kohane, D. S. (2008). Hydrogels in drug delivery: Progress and challenges. *Polymer, 49*, 1993–2007. https://doi.org/10.1016/j.polymer.2008.01.027

Homaeigohar, S., & Boccaccini, A. R. (2022). Nature-derived and synthetic additives to poly(ε-Caprolactone) nanofibrous systems for biomedicine; an updated overview. *Frontiers in Chemistry, 9*. https://doi.org/10.3389/fchem.2021.809676

Jalvo, B., Mathew, A. P., & Rosal, R. (2017). Coaxial poly(lactic acid) electrospun composite membranes incorporating cellulose and chitin nanocrystals. *Journal of Membrane Science, 544*, 261–271. https://doi.org/10.1016/j.memsci.2017.09.033

Kim, M. S., Park, S. J., Gu, B. K., & Kim, C.-H. (2012). Polycaprolactone-chitin nanofibrous mats as potential scaffolds for tissue engineering. *Journal of Nanomaterials*. , Article 635212. https://doi.org/10.1155/2012/635212, 2012.

Li, H., Sanchez-Vazquez, B., Trindade, R. P., Zou, Q., Mai, Y., Dou, L., Zhu, L.-M., & Williams, G. R. (2019). Electrospun oral formulations for combined photo-chemotherapy of colon cancer. *Colloids Surfaces B Biointerfaces, 183*, Article 110411. https://doi.org/10.1016/j.colsurfb.2019.110411

Lima, E., Barroso, A. G., Sousa, M. A., Ferreira, O., Boto, R. E., Fernandes, J. R., Almeida, P., Silvestre, S. M., Santos, A. O., & Reis, L. V. (2022). Picolylamine-functionalized benz[e]indole squaraine dyes: Synthetic approach, characterization and in vitro efficacy as potential anticancer phototherapeutic agents. *European Journal of Medicinal Chemistry, 229*, Article 114071. https://doi.org/10.1016/j.ejmech.2021.114071

Lima, E., Ferreira, O., Gomes, V. S. D., Santos, A. O., Boto, R. E., Fernandes, J. R., Almeida, P., Silvestre, S. M., & Reis, L. V. (2019). Synthesis and in vitro evaluation of the antitumoral phototherapeutic potential of squaraine cyanine dyes derived from indolenine. *Dyes and Pigments, 167*, 98–108. https://doi.org/10.1016/j.dyepig.2019.04.007

Lima, E., Ferreira, O., Oliveira, J. M., Boto, R. E., Fernandes, J. R., Almeida, P., Silvestre, S. M., Santos, A. O., & Reis, L. V. (2025). From darkness to radiance": Light-induced type I and II ROS-mediated apoptosis for anticancer effects of dansylpiperazine-bearing squaraine dyes. *Bioorganic Chemistry, 159*, Article 108379. https://doi.org/10.1016/j.bioorg.2025.108379

Lima, E., Ferreira, O., Silva, J. F., Santos, A. O., Boto, R. E., Fernandes, J. R., Almeida, P., Silvestre, S. M., & Reis, L. V. (2020). Photodynamic activity of indolenine-based aminosquaraine cyanine dyes: Synthesis and in vitro photobiological evaluation. *Dyes and Pigments, 174*, Article 108024. https://doi.org/10.1016/j.dyepig.2019.108024

Lima, E., & Reis, L. V. (2022). Lights, squaraines, action!" - the role of squaraine dyes in photodynamic therapy. *Future Medicinal Chemistry, 14*, 1375–1402. https://doi.org/10.4155/fmc-2022-0112

Lima, E., & Reis, L. V. (2023). Photodynamic therapy: From the basics to the current progress of N-heterocyclic-bearing dyes as effective photosensitizers. *Molecules*, 28. https://doi.org/10.3390/molecules28135092

Lobo, C. S., Mendes, M. I. P., Pereira, D. A., Gomes-da-Silva, L. C., & Arnaut, L. G. (2023). Photodynamic therapy changes tumour immunogenicity and promotes immune-checkpoint blockade response, particularly when combined with micromechanical priming. *Scientific Reports, 13*, Article 11667. https://doi.org/10.1038/s41598-023-38862-8

Ma, F., Yuan, C.-W., Ren, X.-X., You, C.-J., Cao, J.-H., & Wu, D.-Y. (2018). 5,10,15,20-Tetrakis (4-carboxyphenyl) porphin-conjugated poly(l-lactic) acid/polyethylene oxide nanofiber membranes for photodynamic therapy. *Journal of Photochemistry and Photobiology. A, Chemistry, 355*, 267–273. https://doi.org/10.1016/j.jphotochem.2017.08.062

Niemczyk-Soczynska, B., Gradys, A., & Sajkiewicz, P. (2020). Hydrophilic surface functionalization of electrospun nanofibrous scaffolds in tissue engineering. *Polymers*, 12. https://doi.org/10.3390/polym12112636

Niknam, Z., Golchin, A., Rezaei-Tavirani, M., Ranjbarvan, P., Zali, H., Omidi, M., & Mansouri, V. (2022). Osteogenic differentiation potential of adipose-derived mesenchymal stem cells cultured on magnesium oxide/polycaprolactone nanofibrous scaffolds for improving bone tissue reconstruction. *Advanced Pharmaceutical Bulletin, 12*, 142–154. https://doi.org/10.34172/apb.2022.015

Oliveira, A. S., Ferreira, L. F. V., Worrall, D. R., & Wilkinson, F. (1996). Photophysics of oxacyanine dyes on surfaces. Re-examination of the origins of the 'new emission' observed with laser excitation and high concentrations of adsorbed dyes. *Journal of the Chemical Society, Faraday Transactions, 92*, 4809–4814. https://doi.org/10.1039/FT9969204809

Panda, P. K., Hsieh, C.-Y., Shen, Y.-T., Tsai, Y.-H., Tsai, H.-W., Yao, C.-L., Chen, Y., & Yang, P.-C. (2024). Synthesis and physicochemical properties of doxorubicin-loaded PEGA containing amphiphilic block polymeric micelles. *Journal of Polymer Research, 31*, 306. https://doi.org/10.1007/s10965-024-04153-7

Pereira, A. G. B., Fajardo, A. R., Gerola, A. P., Rodrigues, J. H. S., Nakamura, C. V., Muniz, E. C., & Hsieh, Y.-L. (2020). First report of electrospun cellulose acetate nanofibers mats with chitin and chitosan nanowhiskers: Fabrication, characterization, and antibacterial activity. *Carbohydrate Polymers, 250*, Article 116954. https://doi.org/10.1016/j.carbpol.2020.116954

Qin, X., Wu, Y., Liu, S., Yang, L., Yuan, H., Cai, S., Flesch, J., Li, Z., Tang, Y., Li, X., Zhuang, Y., You, C., Liu, C., & Yu, C. (2021). Surface modification of polycaprolactone scaffold with improved biocompatibility and controlled growth factor release for enhanced stem cell differentiation. *Frontiers in Bioengineering and Biotechnology, 9*, Article 802311. https://doi.org/10.3389/fbioe.2021.802311

Rafael, D., Melendres, M. M. R., Andrade, F., Montero, S., Martinez-Trucharte, F., Vilar-Hernandez, M., Durán-Lara, E. F., Schwartz Jr, S., & Abasolo, I. (2021). Thermo-responsive hydrogels for cancer local therapy: Challenges and state-of-art. *International Journal of Pharmaceutics, 606*, Article 120954. https://doi.org/10.1016/j.ijpharm.2021.120954

Ribeiro, A. S., Costa, S. M., Ferreira, D. P., Abidi, H., & Fangueiro, R. (2021a). Development of chitosan-gelatin nanofibers with cellulose nanocrystals for skin protection applications. *Key Engineering Materials, 893*, 45–55. https://doi.org/10.4028/www.scientific.net/KEM.893.45

Ribeiro, A. S., Costa, S. M., Ferreira, D. P., Calhelha, R. C., Barros, L., Stojković, D., Soković, M., Ferreira, I. C. F. R., & Fangueiro, R. (2021b). Chitosan/nanocellulose electrospun fibers with enhanced antibacterial and antifungal activity for wound dressing applications. *Reactive & Functional Polymers, 159*, Article 104808. https://doi.org/10.1016/j.reactfunctpolym.2020.104808

Rohani Shirvan, A., Hemmatinejad, N., Bahrami, S. H., & Bashari, A. (2021). A comparison between solvent casting and electrospinning methods for the fabrication of neem extract-containing buccal films. *Journal of Industrial Textiles, 51*, 311S–335S. https://doi.org/10.1177/15280837211027785

Sarbadhikary, P., George, B. P., & Abrahamse, H. (2021). Recent advances in photosensitizers as multifunctional theranostic agents for imaging-guided photodynamic therapy of cancer. *Theranostics, 11*, 9054–9088. https://doi.org/10.7150/thno.62479

Sayin, S., Tufani, A., Emanet, M., Genchi, G. G., Sen, O., Shemshad, S., … Ozaydin Ince, G. (2019). Electrospun nanofibers with pH-responsive coatings for control of release kinetics. *Frontiers in Bioengineering and Biotechnology, 7*, 309. https://doi.org/10.3389/fbioe.2019.00309

Severyukhina, A. N., Petrova, N. V., Smuda, K., Terentyuk, G. S., Klebtsov, B. N., Georgieva, R., Baumler, H., & Gorin, D. A. (2016). Photosensitizer-loaded electrospun chitosan-based scaffolds for photodynamic therapy and tissue engineering. *Colloids and Surfaces B: Biointerfaces, 144*, 57–64. https://doi.org/10.1016/j.colsurfb.2016.03.081

Shen, J., Yuan, W., Badv, M., Moshaverinia, A., & Weiss, P. S. (2023). Modified poly (ε-caprolactone) with tunable degradability and improved biofunctionality for regenerative medicine. *ACS Materials Au, 3*, 540–547. https://doi.org/10.1021/acsmaterialsau.3c00027

Şimşek, M. (2020). Tuning surface texture of electrospun polycaprolactone fibers: Effects of solvent systems and relative humidity. *Journal of Materials Research, 35*, 332–342. https://doi.org/10.1557/jmr.2020.20

Tabakoglu, S., Kołbuk, D., & Sajkiewicz, P. (2023). Multifluid electrospinning for multi-drug delivery systems: Pros and cons{,} challenges{,} and future directions. *Biomaterials Science, 11*, 37–61. https://doi.org/10.1039/D2BM01513G

Tseng, Y.-Y., Liao, J.-Y., Chen, W.-A., Kao, Y.-C., & Liu, S.-J. (2013). Sustainable release of carmustine from biodegradable poly[(d,l)-lactide-co-glycolide] nanofibrous membranes in the cerebral cavity: In vitro and in vivo studies. *Expert Opinion on Drug Delivery, 10*, 879–888. https://doi.org/10.1517/17425247.2013.758102

Wang, L., Ezazi, N. Z., Liu, L., Ajdary, R., Xiang, W., Borghei, M., Santos, H. A., & Rojas, O. J. (2020). Microfibers synthesized by wet-spinning of chitin nanomaterials: Mechanical, structural and cell proliferation properties. *RSC Advances, 10*, 29450–29459. https://doi.org/10.1039/D0RA06178F

WHO (WHO). (2022). Cancer. https://www.who.int/news-room/fact-sheets/detail/cancer accessed October 3, 2023.

Xiang, S., Zhang, X., Cao, Z., Peng, S., Xu, J., Huang, Q., Huang, J., Xu, C., & Sun, X. (2024). Comparing the antibacterial activity of chitin nanocrystals with chitin: Exploring the feasibility of chitin nanocrystals as novel pesticide nanocarriers in agriculture. *Pest Management Science, 80*, 1076–1086. https://doi.org/10.1002/ps.7838

Yang, X., Liu, J., Pei, Y., Zheng, X., & Tang, K. (2020). Recent progress in preparation and application of nano-chitin materials. *ENERGY \& Environ. Mater, 3*, 492–515. https://doi.org/10.1002/eem2.12079

Zhong, T., Wolcott, M. P., Liu, H., & Wang, J. (2020). Propionylation-modified chitin with improved solubility in green ethanol/water binary solvents for sustainable film and coating applications. *Journal of Cleaner Production, 250*, Article 119458. https://doi.org/10.1016/j.jclepro.2019.119458